Accepted Manuscript

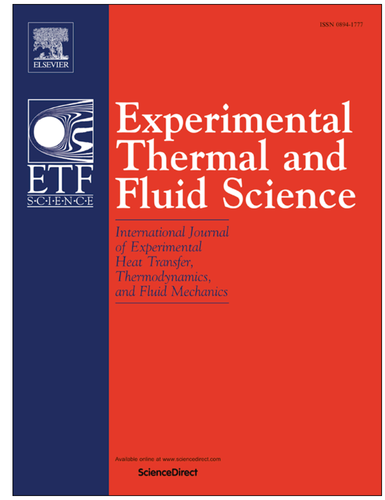

Local dissipation scales in turbulent jets

Minyi Xu, Kin-Pang Cheong, Jianchun Mi, Andrew Pollard

PII: S0894-1777(17)30402-8
DOI: https://doi.org/10.1016/j.expthermflusci.2017.12.019
Reference: ETF 9309

To appear in: *Experimental Thermal and Fluid Science*

Received Date: 12 July 2017
Revised Date: 14 November 2017
Accepted Date: 21 December 2017

Please cite this article as: M. Xu, K-P. Cheong, J. Mi, A. Pollard, Local dissipation scales in turbulent jets, *Experimental Thermal and Fluid Science* (2017), doi: https://doi.org/10.1016/j.expthermflusci.2017.12.019

Local dissipation scales in turbulent jets

Minyi Xu [a)], Kin-Pang Cheong[b)], Jianchun Mi [b) †], Andrew Pollard [c) †],

a) Marine Engineering College, Dalian Maritime University, Dalian, 116026, China

b) State Key Laboratory of Turbulence & Complex Systems, College of Engineering, Peking University, Beijing 100871, China

c) Department of Mechanical and Materials Engineering, Queen's University at Kingston, Ont., K7L 3N6, Canada

Abstract: This work characterizes the local dissipation length-scale η and its related quantities in turbulent (round and square) jets. It is revealed that the probability density function (PDF) of η, denoted by $Q(\eta)$, displays different shapes in the jet's central region and shear layer. In the central jet of full turbulence, the distribution of $Q(\eta)$ is insensitive to changes in the initial flow conditions and the degree of anisotropy, and agrees well with those obtained previously from a pipe flow and DNS of a box turbulence. On the other hand, the left tail of $Q(\eta)$ at small η rises with increasing lateral distance from the centerline (towards the jet outer region), where the turbulent/non-turbulent intermittency occurs due to jet engulfment of ambient fluid; such large-scale intermittency is expected to enhance fine-scale dissipation intermittency. Therefore, the present work demonstrates that the smallest-scale dissipation fluctuations behave universally as in fully turbulent flows, irrespective of the flow type; but this universality is broken in partially turbulent flows or in flow regions where large-scale intermittency emerges.

Keywords: Turbulent jet; Local dissipation scales; Intermittency; Engulfment

† Corresponding authors: J. Mi (jmi@pku.edu.cn); A. Pollard (andrew.pollard@queensu.ca)

1. Introduction

Turbulence is characterized by velocity fluctuations on a wide range of scales and frequencies [1, 2]. In the classical theory of turbulence [3], the turbulent kinetic energy transfers continuously from large to small scales, and would end at the smallest length scale of turbulence, known as the Kolmogorov dissipation scale $\eta_K \equiv (\nu^3/<\varepsilon>)^{1/4}$. Here, ν is the kinematic viscosity of the fluid and $<\varepsilon>$ is the mean energy dissipation rate, which equals to the average flux of energy from the energy-containing large-scale eddies down to the smallest ones in the case of statistically stationary turbulent fluid motion [3]. However, the dissipation field $\varepsilon(\boldsymbol{x},t) = (\nu/2)(\partial_i u_j + \partial_j u_i)^2$ is driven by fluctuations of velocity gradients whose magnitudes exhibit intense spikes in both space and time, resulting in spatially intermittent regions of high turbulent dissipation within a turbulent flow field [4-6]. Here, the variable u_i is the fluctuating velocity. The Kolmogorov dissipation length η_K is obtained from the time-averaged $<\varepsilon>$ that does not account for the strongly intermittent nature of the dissipation rate field.

To examine the intermittency of $\varepsilon(\boldsymbol{x},t)$, Paladin and Vulpiani [7] put forward the idea of a local dissipation length scale η, together with a local Reynolds number of order 1 that is defined as $\mathrm{Re}_\eta = \eta\left|\delta_\eta u\right|/\nu$. Here, $\delta_\eta u = u(x+\eta) - u(x)$ is the longitudinal velocity increment over a separation of η. This local Reynolds number means that the inertial force $(\delta_\eta u)^2/\eta$ and the viscous force $\nu\left|\delta_\eta u\right|/\eta^2$ are local and instantaneously balanced. To the dissipation scale η, all contributions from pressure, advection and the dissipation terms are assumed to be of the same order [8]. Physically, η can be interpreted as the instantaneous cut-off scale where viscosity overwhelms inertia. To capture the dynamics of the dissipation structures, the continuous distribution of dissipation scales represented by its probability density function (PDF), $Q(\eta)$, was also theoretically (e.g., [8, 9]) and numerically (e.g., [10, 11]) investigated. Assuming that the energy flux toward small scales begins at the integral length-scale L and that the PDF of velocity increments $\delta_L u$ ($\equiv u(x+L) - u(x)$) is close to Gaussian, Yakhot derived an analytical form for $Q(\eta)$ by applying the Mellin transform to the structure function exponent relationships for moments of $\delta_\eta u$ within the range $0 < \eta < L$ as,

$$Q(\eta) = \frac{1}{\pi\eta(b\log(L/\eta))^{1/2}} \int_{-\infty}^{\infty} dx \times \exp[-x^2 - \frac{(\log(\sqrt{2}\,\mathrm{Re}_L(\eta/L)^{a+1}))^2}{4b\log(L/\eta)}] \tag{1}$$

where a = 0.383, b = 0.0166 as in Ref. [10]. Yakhot showed that the scales η form a random field not necessarily related to the energy dissipation scales but rather to the linear dimensions of various dissipation structures defined by the local value of Reynolds number. Thus, the scale η must be perceived as a dynamics cut-off separating analytic and singular components of the velocity field.

Bailey et al. [6] experimentally obtained $Q(\eta)$ using data from a turbulent pipe flow over a wide range of Reynolds numbers. Their results agree well with those from high resolution numerical simulations of homogeneous and isotropic box turbulence [10], but not so well with Eq. (1), which suggests a universal behavior of the smallest-scale fluctuations around the Kolmogorov dissipation scale. To test the universality of the smallest-scale fluctuations in different flows, Zhou and Xia [12, 13], and Qiu et al. [14] investigated the $Q(\eta)$ in Rayleigh–Bénard convection and Rayleigh-Taylor turbulence, respectively. Their results revealed that the PDF distributions of η are indeed insensitive to large-scale inhomogeneity and anisotropy of the system, and confirmed that the small-scale dissipation dynamics can be described by the same models developed for homogeneous and isotropic turbulence. However, the exact functional form of $Q(\eta)$ is not universal with respect to different types of flows. In the presence of strong mean shear, e.g., wall bounded turbulent shear flow [11], and the flow past a backward facing step [15], the peaks of $Q(\eta)$ were found to shift along the η axis in portions of the log-layer and the buffer layer. This departure was attributed to the specific properties of near wall coherent structures. Recently, Bailey et al. [16] examined the Re and mean shear dependence of $Q(\eta)$ for channel flow and found that much of the previously observed spatial dependence can be attributed to how the results are normalized.

Although the properties of $Q(\eta)$ have been investigated in several types of flows, these ideas have not been tested in turbulent jet flows, which are widely used in various industrial mixing processes ([4, 17-22]). In jet flows, the ambient fluid is engulfed into the main jet, resulting in "large-scale intermittency" or "external intermittency", which is related to the turbulent/non-turbulent interfaces [23, 24]. The large-scale intermittency was found to have stronger influence on the spectral inertial-range exponent than the mean shear rate. In this context, the present study is designed through two jet flows to address the following two issues:

(1) Does the smallest-scale dissipation fluctuations behave universally alike in fully turbulent flows?

(2) If so, does this universality remain valid in partially turbulent flows or flow region where large-scale intermittency emerges?

The remainder of this paper is organized as follows. Section 2 provides the experimental details of the two jets considered: one round jet and one that emanates from a long square sectioned duct. The behavior of local dissipation scales and the local velocity increments are presented and discussed in Section 3, including the effects of mean shear and large scale intermittency. Finally, conclusions are drawn in Section 4.

2. Description of the experiments

Experimental details for the round and square jets are given in, and the reader is directed to, Refs [17] and [25], respectively. Here a brief overview is provided. The round jet was generated from a smooth contraction nozzle with a diameter of $D_e = 2$ cm while the square jet issued from a square duct of dimensions 2.5 cm × 2.5 cm × 2 m, with the equivalent diameter of D_e [$\equiv 2(A/\pi)^{1/2}$] ≈ 2.82 cm. For the round jet, the exit velocity U_j = 3 ~ 15 m/s, which corresponds to Re [$\equiv U_j D_e/\nu$] ≈ 6750 ~ 20100; and for the square jet, U_j = 4.2 ~ 26.4 m/s and Re = 8×10^3 ~ 5×10^4. Note that the round jet Re is marginally fully turbulent, as defined by the mixing transition, see Refs. [26]. For both jets, the streamwise velocity was measured using single hot-wire anemometry.

The properties of small-scale turbulence were obtained using the digital filtering high-frequency noise scheme proposed by Mi et al. [27]. The dissipation and mean-square fluctuation derivatives were corrected following Hearst *et al.* [28]. The present hotwire probe has a limited resolution due to its finite spatial dimensions and temporal response. Specifically, its resolution was determined by the wire diameter d_w = 5 μm and effective length $\ell_w \approx 1$ mm, plus its response frequency and sampling rate during measurements. Note that the ratio $\ell_w/d_w \approx 200$ is required so that both a nearly uniform temperature distribution in the central portion of the wire and a high sensitivity to flow velocity fluctuations can be achieved [29]. The present study corrected the spatial attenuation n of the single wire due to $\ell_w \approx 1$ mm using the procedure of Wyngaard [30], which was developed in spectral space to account for the integration effect on Fourier components of the velocity.

When Re = 20100 for the round jet, for instance, the time difference varies from Δx = 0.27 mm at x/d = 19 to Δx = 0.17 mm at x/d = 33. By comparison, the corresponding value of the Kolmogorov scale was estimated to be $\eta_K \approx 0.09$ mm at

x/d = 19 to $\eta_K \approx 0.15$ mm at x/d = 33, from the corrected dissipation rates. Furthermore, Bailey et al. [6] showed that the measured PDFs of the local dissipation scales Q(η) are expected to be largely insensitive to the influence of spatial filtering and instrumentation noise. In the present study, the insensitivity of the results to changing Reynolds number and Kolmogorov length scale η_K as provided in Fig. 1 further confirms this expectation.

The present measurements consider the radial distributions of the local dissipation and probability density functions of the integral length scale. These span $0 < y/y_{1/2} < 1.7$, which introduces some large scale intermittency into the signals. It has been demonstrated by Sadeghi et al.[31] that data obtained (and suitably corrected as above) using a stationary hot wire depart from those obtained in the same flow using a flying hot wire for $y/y_{1/2} > 1$.

The PDFs of η were calculated from each velocity time series, $u(t)$, using the procedure as described in Refs [6, 11, 12]. First, the velocity difference $\Delta u(\Delta t) = |u(t+\Delta t) - u(t)|$ was calculated at each discrete time t by assuming $r_1 \approx \langle U \rangle \Delta t$. Next, for each t, the local Reynolds number $Re_\eta = \Delta u(\Delta t) r_1/\nu$ was calculated at $0 < \psi r_1 < \psi 4L$ while each instance when $Re_\eta = 0.9 \sim 2$ was counted as a single occurrence of dissipation at a scale $\eta = r_1$. This process was repeated for all Δt to generate Q(η). Here, the integral length scale $L = U_c T = U_c \int_0^{\tau_0} \langle u(t)u(t+\tau) \rangle \langle u^2 \rangle^{-1} d\tau$, where τ_0 corresponding to the first zero crossing of the autocorrelation function $\langle u(t)u(t+\tau) \rangle$. Finally Q(η) was obtained by normalization such that $\int Q(\eta) d\eta = 1$.

3. Presentation and Discussion of Results

3.1 PDFs of local dissipation scales and velocity increments along the jet centreline

The PDFs of local dissipation scale obtained on the jet centerline at x/D_e = 1, 5 and 30 for both the round and square jets for all the Reynolds numbers are presented in Figure 1 (a) and (b), where $Q(\eta)$ is normalized by $\eta_0 = LRe_L^{-0.72}$ and $\mathrm{Re}_L = <|u_x(x+L) - u_x(x)|^2>^{1/2}L/\nu$ [6, 12]. For comparison, the results from the box turbulence [10], pipe flow [6], Rayleigh–Bénard convection [12] and theoretical distribution [8] are also displayed.

The distributions obtained in the near and far field regions of the jet flows coincide very well with each other over all measured scales. Note that the round jet was generated from a smooth contraction nozzle while the square jet issued from a long pipe, i.e., their initial conditions are quite different. The agreement seems independent of nozzle type and exit Reynolds number. This result is somewhat unexpected and surprising for many reasons.

It is well known that the vorticity layer arising from the nozzle inner wall becomes unstable, forming Kelvin–Helmholtz waves and then forming vortex rings that convect downstream. These organized vortex rings eventually break down into more complex coherent structures within a few diameters of the jet nozzle (x/D_e <5). As the flow develops downstream, the fluid entrainment becomes more stochastic in the central flow region, where incoherent small-scale turbulence plays a critical role, than in the outer region, where large-scale coherent motion dominates. There is ample evidence to indicate isotropy on the centreline in the far-field [22]. According to previous studies [17, 22], both the large-scale and small-scale turbulent statistics (e.g., mean velocity decay, turbulent intensity, mean energy dissipation rate, Kolmogorov scale) in the two jets should behave somewhat differently. However, the centerline $Q(\eta)$ of jet flows appears to be independent of initial conditions.

Additionally, the Re considered for both jets brackets the mixing transition Reynolds number of about 20,000 so that both spatial effects (*i.e.* 1<x/De<30) and Re effects should be expected to be observed, see Fellouah and Pollard [26], not to mention the inlet conditions are markedly different with the square jet containing secondary flows that arise from the anisotropic stress field. That all data agree with those from the centerline of the pipe flow of Bailey et al. [6] tends to reinforce the universality of the distribution of $Q(\eta)$.

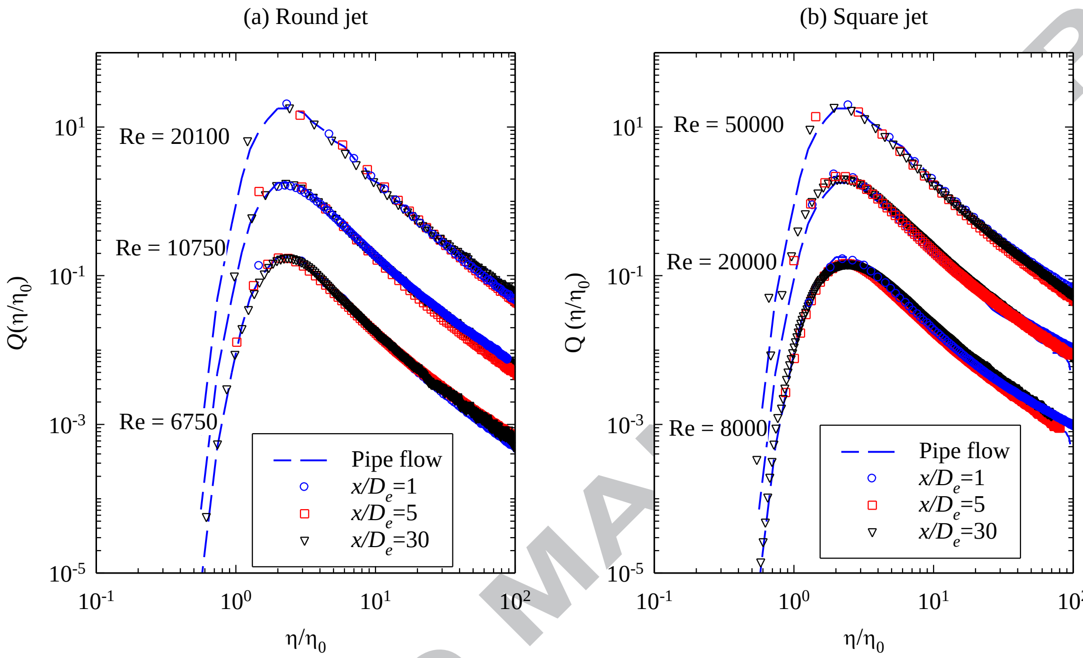

Figure 1 Centerline PDFs of the local dissipation scale obtained at x/De = 1, 3 and 30 in (a) the round jet and (b) the square jet for all the Reynolds numbers. For clarity, results for the two high Reynolds numbers are shifted upward by one and two decades, respectively. Results from the centerline of pipe flow [6] at Re = 24000 are also included.

In theoretical approaches [8] and numerical simulations of isotropic turbulence [10, 11], it is usually assumed that the PDF of velocity increments $\delta_L u$ ($\equiv u(x+L)$ - $u(x)$) across the integral length scale L are Gaussian distributed, *i.e.*, P($\delta_L u$) ~ exp(-$\delta_L u^2$/2). Such an assumption, that the PDF is Gaussian, has been verified on the centreline of jet flows. Figure 2 presents P($\delta_L u$) measured along the centreline of the two jets. The Gaussian distribution is also given for reference. Notably, the tails of the PDFs display a slight lack of adherence to the Gaussian, which in the case of the round jet may be due to the Re being on the cusp of reaching fully developed turbulence, as embrassed by in the mixing transition argument [18, 26]. However, the excellent agreement of the centerline $Q(\eta)$ of the jet flows, pipe flow and box turbulence indicates that the smallest-scale fluctuations in fully turbulence are universal, and independent of the turbulent flow conditions and the degree of anisotropy.

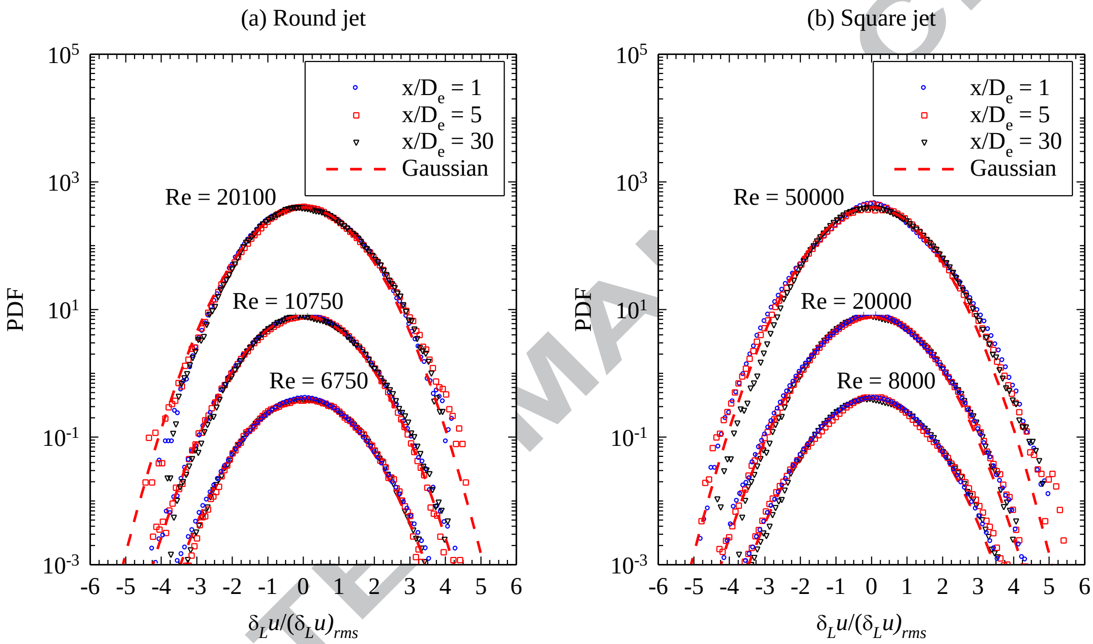

Figure 2 PDFs of $\delta_L u = u(x+L) - u(x)$ on the centreline for x/D_e = 1, 5 and 30 for (a) the round jet and (b) the square jet at different Re. Gaussian distributions are also added for reference.

3.2 PDFs of local dissipation scales and velocity increments across the shear layer

In this portion of the paper, the distributions of $Q(\eta)$ across the jet radii are considered. As noted above, Sadeghi and Pollard [31] found that for $y/y_{1/2} > 1$ or so, the stationary hot wire data departed from those obtained using a flying hot wire. This is due to inhomogeneity and reversed flow encountered by the stationary wire. Thus, the results to be presented in this section of the paper must be viewed with some skepticism for regions beyond $y/y_{1/2} = 1$.

Figures 3 (a) and 3(b) present the log-log plots of $Q(\eta)$, respectively, for the round jet at Re = 20100 and square jet at Re = 50000, measured for $x/D_e = 30$ and at the three lateral locations indicated on the plots. For comparison, the results from the box turbulence[10], pipe flow[6], Rayleigh－Bénard convection[12] and theoretical distribution [8] are also displayed. Evidently, the distributions of $Q(\eta)$ for $y/y_{1/2} = 0$ and 0.9 in the round jet, as well as those for $y/y_{1/2} = 0$ and 0.8 in the square jet, collapse over the whole range of η/η_o. Also, the PDFs from all the measurement locations collapse well for $\eta/\eta_o \geq 1.5$, irrespective of the square or round jet. However, it appears that, for $\eta/\eta_o < 1.5$, $Q(\eta)$ increases with increasing y at $y/y_{1/2} \geq 1$. This is perhaps a manifestation of the increased level of small-scale intermittency in the jet outer region where non-turbulence occurs frequently due to large-scale jet engulfment of irrotational ambient fluid.

Comparison is also made in Fig. 3 between the results of the present jets, the box turbulence [10], pipe flow [6], Rayleigh－Bénard convection [12] and theoretical distribution [8]. It is very interesting to find that the central-jet data at $y/y_{1/2} < 0.9$ agree very well with the results of pipe flow and box turbulence. However, with further increasing $y/y_{1/2}$ from 0.9, the left tail of $Q(\eta)$ gradually increases at small η, indicating the increased level of small-scale intermittency at these scales. Such higher probabilities at small η is also observed in Rayleigh–Bénard convection [12] due to the presence of thermal plumes, but the exact function form of $Q(\eta)$ in Rayleigh–Bénard convection is found to be universal at different representative locations. Also evidently in Fig.3, the deviations between the $Q(\eta)$ measured in the present two jet flows and the theoretical distribution can be due to the limits of a saddle-point approximation for the evaluation of the Mellin transform in [8]. Therefore, such discrepancy suggests that the exact functional form of $Q(\eta)$ should not be considered universal even in the same turbulent flows. The universality of the local dissipation scales in jet flows is found to be disturbed by the large-scale intermittency associated to the engulfment, as discussed in Section 3.3.

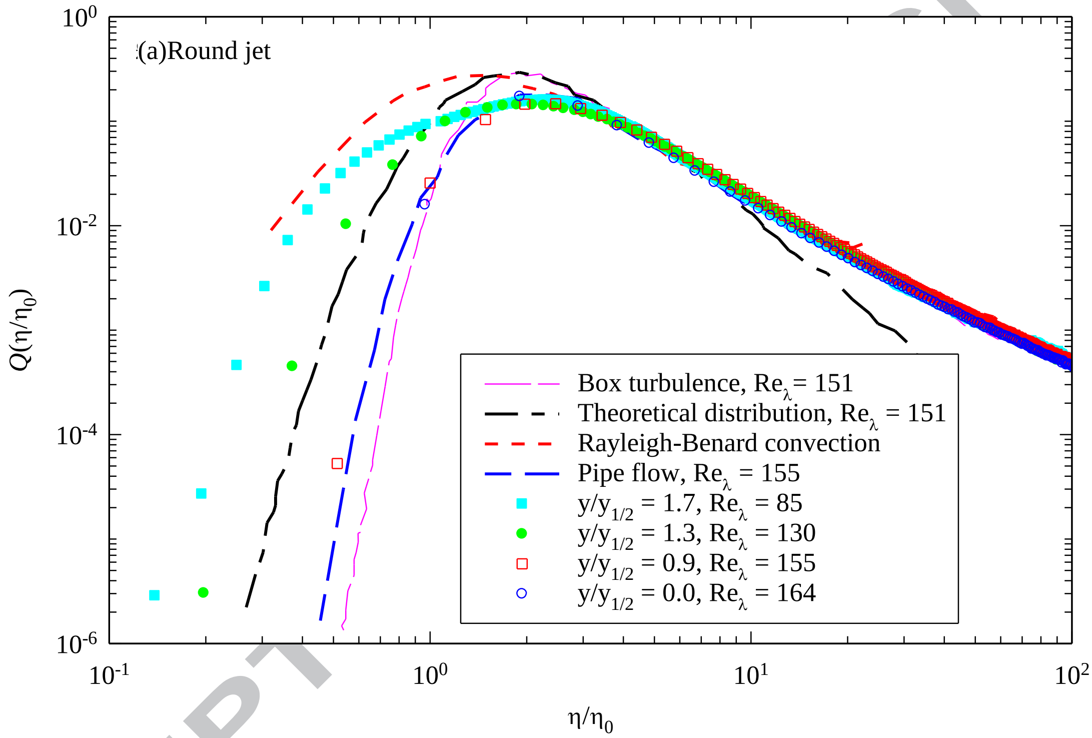

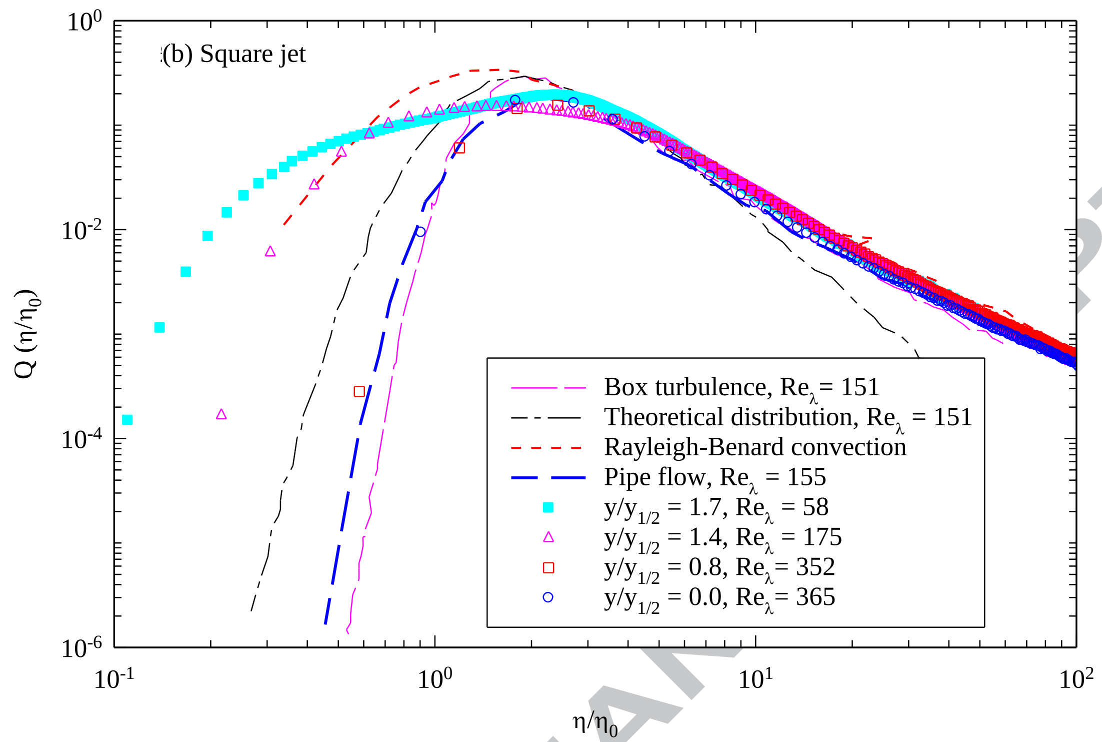

Figure 3. Measured PDFs of the local dissipation scales in the shear layer: (a) round jet at Re = 20100; (b) square jet at Re = 50000. For comparison, the results from the box turbulence[10], pipe flow [6], Rayleigh－Bénard convection [12] and theoretical distribution [8] are also displayed.

Figure 4 shows P($\delta_L u$) measured at x/D_e = 30 in the shear layer of the two jets. Gaussian and exponential distributions are also given for reference. The measured PDFs of $\delta_L u$ at $y/y_{1/2}$ < 0.9 are observed to be closely Gaussian, *i.e.*, P($\delta_L u$) ~ exp($-\delta_L u^2/2$), which was also observed by Renner et al. [32]. However, at $y/y_{1/2}$ > 0.9, the PDFs of $\delta_L u$ gradually exhibit exponential tails, indicating a significant probability for the existence of much larger values than its root mean square value.

Combining the observations from Figs. 3 and 4, we may correlate the left departure of $Q(\eta)$ to the variation of P($\delta_L u$) from near-Gaussian to exponential distribution. This supports that the exact function of $Q(\eta)$ depends on the integral-scale velocity boundary condition. As the buoyancy force governing the cascade dynamics above the so-called Bolgiano scale and the Bolgiano timescale is only a factor of 2 or 3 smaller than the integral timescale, Zhou and Xia [12] claimed that P($\delta_L u$) exhibiting exponential tails may come from the buoyancy-induced intermittency, which is then transferred from large to small scales.

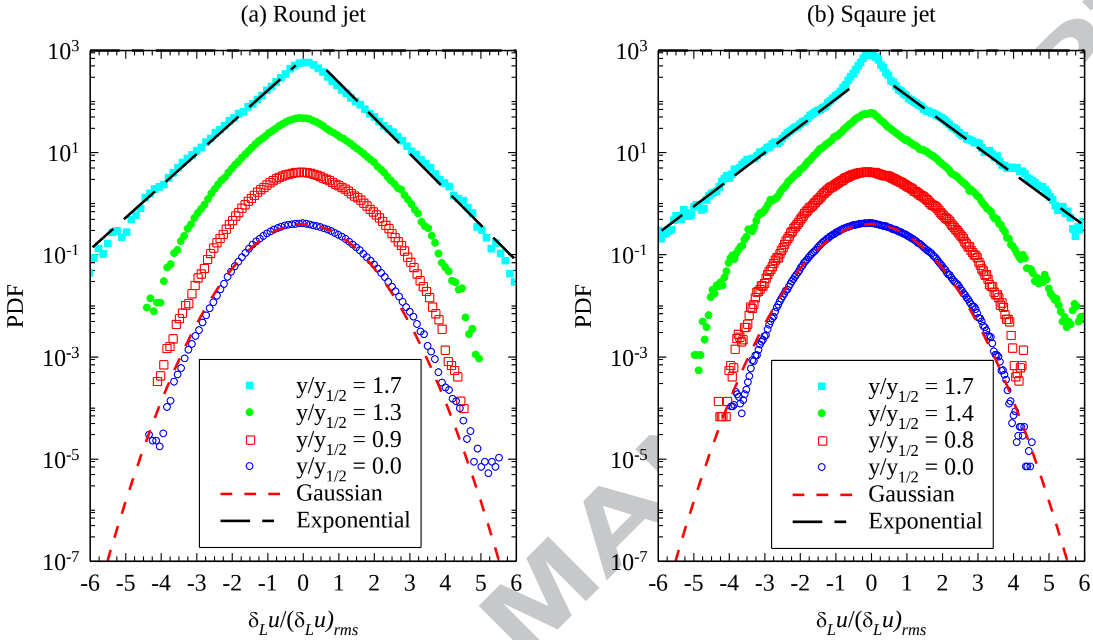

Figure 4. PDFs of $\delta_L u = u(x+L) - u(x)$ in (a) the round jet at Re = 20100 and (b) the square jet at Re = 50000. The PDFs are normalized to their respective standard deviations and shifted in the vertical direction for clarity of presentation. Gaussian and exponential distributions are shown for reference.

3.3 Effect of large-scale intermittency and mean shear on PDFs of local dissipation scales and velocity increments

To understand the variations of P($\delta_L u$) and $Q(\eta)$ in the shear layer of the two jets, the large-scale or external intermittency factor γ ($\equiv$ the fraction of time when the flow is fully turbulent) and mean shear S ($\equiv |\partial U/\partial y|$) are considered. The turbulent energy recognition algorithm (TERA) method proposed by Falco and Gendrich [33] was applied to estimate the intermittency factor from the velocity signals of the jets. Note that the TERA method was successfully used in our previous work [34] to investigate the effects of external intermittency on the spectral inertial-range exponent m in a turbulent square jet and found that m depends strongly on γ but negligibly on S. Therefore, similar to the previous work [34], the threshold constant was also set as C_0 = 0.04 in the TERA criterion for turbulence and nonturbulence as following,

$$I(t) = \begin{cases} 1, & \langle\left|\frac{u\partial u}{\partial t}\right|\rangle > C_0\left(\frac{u\partial u}{\partial t}\right)_{rms} \qquad (signal\ is\ turbulent) \\ 0, & \langle\left|\frac{u\partial u}{\partial t}\right|\rangle \le C_0\left(\frac{u\partial u}{\partial t}\right)_{rms} \qquad (signal\ is\ nonturbulent) \end{cases}$$

where $(\quad)_{rms}$ means the root mean square (rms) value.

Figure 5 shows lateral distributions of γ across the two jets. For comparison, the result of Mi and Antonia [23] for a round jet is also provided. There is reasonable agreement between the two data sets. In addition, Figure 5 also presents the normalized mean velocity U/U_c and mean shear S^*, which is defined as $S^* = (y_{1/2}/U_c)\left|\partial U/\partial y\right| = (y_{1/2}/U_c)S$.

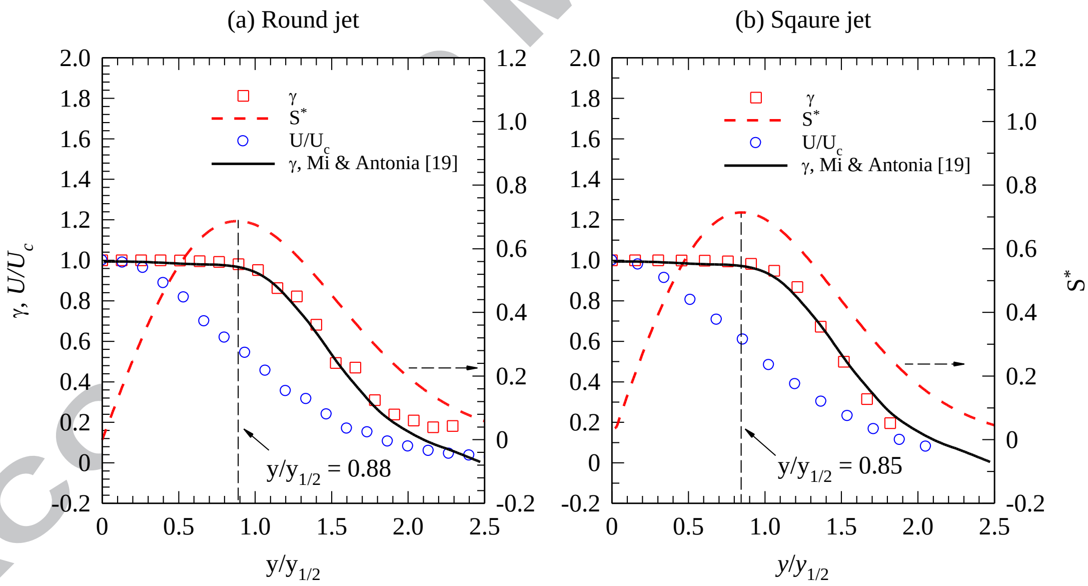

Figure 5 Radial profiles of normalized mean velocity U/U_c, the intermittency factor γ, and mean shear S^* at x/D_e = 30 of (a) the round jet and (b) square jet. The γ data of Mi and Antonia [23] are included for comparison.

Figure 5 indicates that γ ≈ 1 at $0 < y/y_{1/2} < 0.9$. In other words, the flow is fully turbulent in the central region at $y/y_{1/2} < 0.9$. In the same region, the y distributions of

$Q(\eta)$ collapse with those in pipe flow [6] and box turbulence [10], see Fig. 3. In addition, the $P(\delta_L u)$ is nearly Gaussian for $0 < y/y_{1/2} < 0.9$, see Fig.4. This means that the exact function for $Q(\eta)$ is probably universal, while $P(\delta_L u)$ is nearly Gaussian, in the fully turbulent regions of the jets.

Figure 5 also demonstrates that the value of γ decreases quickly from 1 to 0 as $y/y_{1/2}$ increases beyond 0.9, wherein the flow is not always turbulent as some non-turbulent ambient fluid occurs frequently. The interfaces between the non-turbulent and turbulent regions in shear flows were investigated recently [35-37]. The most important feature of this region is the continuous exchange for the transport of heat, mass, and momentum between the irrotational surrounding region and the fully turbulent region of the jet. Therefore, higher values of $Q(\eta)$ at small η in the outer region at $y/y_{1/2} > 0.9$ (Fig. 4) and $P(\delta_L u)$ exhibiting exponential tails (Fig. 5) may be due to the engulfment induced large-scale intermittency.

In addition, Figure 5 shows that the maximum mean shear occurs at $y/y_{1/2} = 0.88$ for the round jet and $y/y_{1/2} = 0.85$ for the square jet. Although there is a strong mean shear rate in the region of full turbulence ($\gamma \approx 1$), the corresponding $Q(\eta)$ still shows excellent agreement with that of the pipe flow, and $P(\delta_L u)$ is Gaussian distributed, see Fig.3 and 4. This evidence suggests that the smallest-scale fluctuations are more sensitive to the intermittency factor γ than the mean shear.

To further investigate the effect of the large-scale intermittency on local dissipation scales, non-turbulent signals are identified and removed from the original velocity signals using the aforementioned TERA algorithm [34]. Samples of the original signals are provided in Fig. 6.

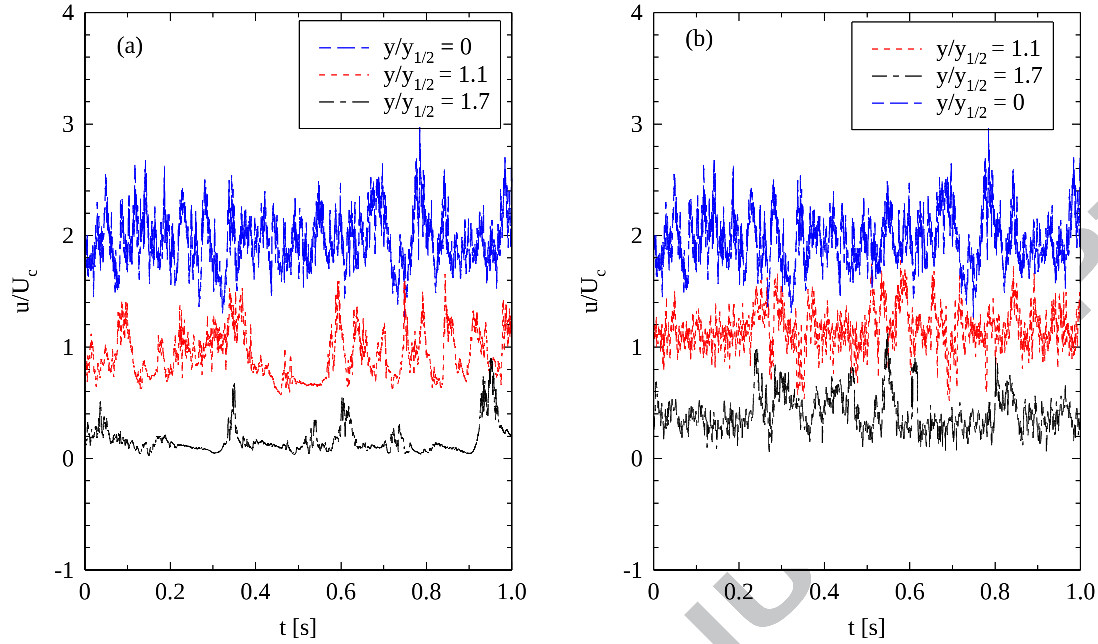

Figure 6 Plots of (a) original velocity signals, and (b) velocity signals excluding the non-turbulent parts using TERA method in the shear layer of the square jet at Re = 50000. The plots for $y/y_{1/2}$=0 and $y/y_{1/2}$=1.1 are shifted 1 and 0.5, respectively.

The revised PDFs of η and $\delta_L u$, estimated from the velocity signals excluding the non-turbulent signals, are presented in Figures 7 and 8, respectively. In Figure 7, it is noted that the $Q(\eta)$ at small η due to the removal of the non-tubulent portion of the signal is lower than the original distributions and approach to those results obtained in the centreline of the two jet flows and pipe flow. The corresponding revised P($\delta_L u$) become nearly Gaussian, see Figure 8.

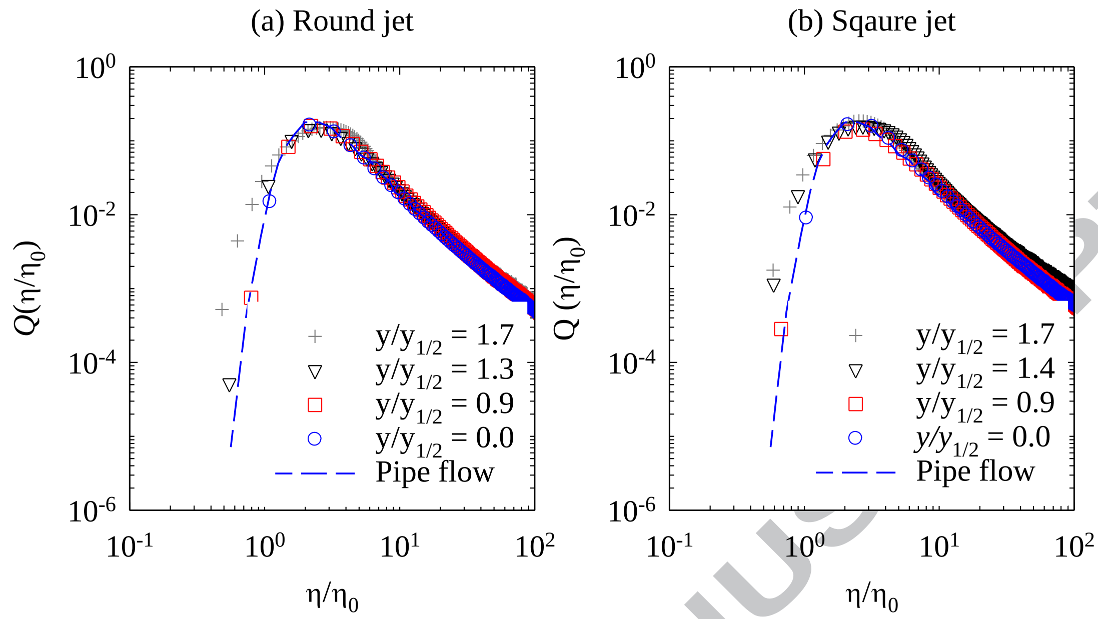

Figure 7 The PDFs of the local dissipation scales estimated from the velocity signals excluding the non-turbulent parts in the shear layer of (a) the round jet and (b) square jet for Re = 20100 and 50000, respectively. The data from pipe flow [6] are also added.

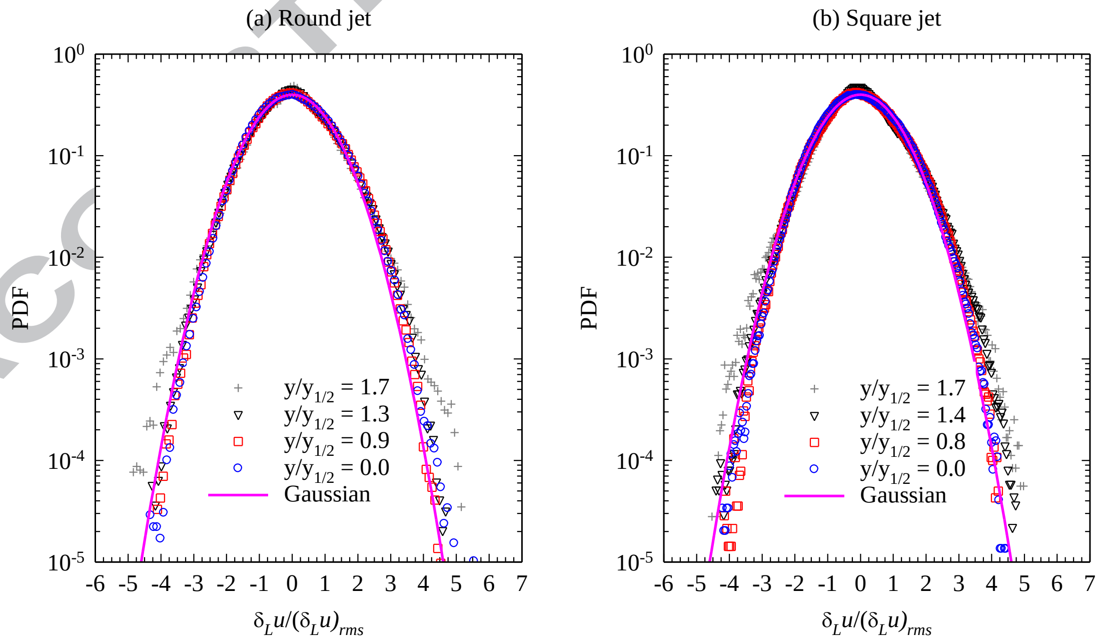

Figure 8 The PDFs of the vertical velocity increments $\delta_L u$, estimated from the

velocity signals excluding the non-turbulent parts in the shear layer of the (a) round jet and (b) the square jet for Re = 20100 and 50000, respectively. Gaussian distribution is also added for reference.

From the above analysis we can induce that the large-scale intermittency associated to engulfment has great impact on the small-scale intermittency of dissipation. The large-scale intermittency factor decreases with more non-turbulent ambient fluid engulfed into main jets. The corresponding large-scale boundary condition, i.e., P($\delta_L u$), gradually exhibits exponential tails, and $Q(\eta)$ exhibit higher probabilities at small local dissipation scale η, indicating the increased level of small-scale intermittency at these scales. The increased level of small-scale intermittency in the shear layer of jet flows is caused by the presence of interface between the turbulence/non-turbulence regions, the size of which in the turbulent round jet is between one-two orders of magnitude smaller than the integral length scale of the flow [37]. Comparably, the large-scale intermittency associated to the large scale coherent motion of thermal plumes in Rayleigh-Benard convection also causes higher probabilities at small dissipation scale η, but the exact function form of $Q(\eta)$ is found to be universal at different representative locations [12]. However, the present results reveal that the universality of the local dissipation scales in jet flows is disturbed by the large-scale intermittency associated to the engulfment. It also suggests that the large scale intermittency factor γ should be considered to derive the exact functional form of Q and PDF of $\delta_L u$ in non- fully turbulent flow.

It is also worth to noting that, in the central jet of full turbulence where the large scale intermittency factor γ is about 1, the present results show that the distribution of $Q(\eta)$ agrees well with those obtained previously from a pipe flow and DNS of a box turbulence and the PDF of $\delta_L u$ is Gaussian. Furthermore, this large-scale intermittency effect is also observed at x/D =1 (not shown here). Thus, this suggests that the $Q(\eta)$ in jet flows is more universal than other small-scale turbulent statistics (e.g., mean velocity decay, turbulent intensity, mean energy dissipation rate, Kolmogorov scale)[17, 22].

4. Conclusions

The present study has investigated the PDF characteristics of the local dissipation length scale η in turbulent round and square jets based on hot-wire measurements. In the central fully-turbulent region, the PDFs of η, $Q(\eta)$, are found to be insensitive to changes of initial flow conditions and the degree of anisotropy, and agree well with those previously measured in fully turbulent pipe flow [6] and calculated from box turbulence [10]. However, in the jet shear layer, $Q(\eta)$ exhibits higher probabilities at small η, indicating the increased level of small-scale intermittency, and the PDF of $\delta_L u$ gradually exhibiting exponential tail from Gaussian. This behavior is expected to result from the presence of a large-scale turbulent/non-turbulent intermittency caused by jet engulfment of the surrounding fluid. Compared to the large-scale intermittency, the mean shear rate and Reynolds number are found to impose negligible influences on $Q(\eta)$. Finally, the present results suggest that the smallest-scale fluctuations behave universally alike only in fully turbulent flows or fully turbulent regions in jet flows. In partially turbulent flows, the smallest-scale fluctuations depend on the large-scale intermittency.

Acknowledgements

The supports of the Nature Science Foundation of China (Grants No. 51506019), the Fundamental Research Funds for the Central Universities, China (Nos. 3132016337, 3132016204) and Young Elite Scientists Sponsorship Program By CAST (2016QNRC001) are gratefully acknowledged.

References

[1] U. Frish, Turbulence: The lengacy of A. N. Kolmogrov, Cambridge University, Cambridge, 1995.
[2] J.C. Vassilicos, Dissipation in Turbulent Flows, Annu. Rev. Fluid Mech., 47 (2015) 95-114.
[3] A.N. Kolmogorov, The Local Structure of Turbulence in Incompressible Viscous Fluid for Very Large Reynolds Numbers, Dokl. Akad. Nauk SSSR, 30 (1941) 301-305.
[4] K.R. Sreenivasan, R.A. Antonia, The phenomenology of small-scale turbulence, Annu. Rev. Fluid Mech., 29 (1997) 435-472.
[5] T. Ishihara, T. Gotoh, Y. Kaneda, Study of high-Reynolds number isotropic turbulence by direct numerical simulation, Annu. Rev. Fluid Mech., 41 (2009) 165-180.
[6] S. Bailey, M. Hultmark, J. Schumacher, V. Yakhot, A. Smits, Measurement of local dissipation scales in turbulent pipe flow, Phys. Rev. Lett., 103 (2009) 14502.
[7] G. Paladin, A. Vulpiani, Anomalous scaling laws in multifractal objects, Phys. Rep., 156 (1987) 147-225.
[8] V. Yakhot, Probability densities in strong turbulence, Physica D: Nonlinear Phenomena, 215 (2006) 166-174.
[9] L. Biferale, A note on the fluctuation of dissipative scale in turbulence, Phys. Fluids, 20 (2008) 031703.
[10] J. Schumacher, Sub-Kolmogorov-scale fluctuations in fluid turbulence, Europhysics Letters, 80 (2007) 54001.
[11] P.E. Hamlington, D. Krasnov, T. Boeck, J. Schumacher, Local dissipation scales and energy dissipation-rate moments in channel flow, J. Fluid Mech., 701 (2012) 419-429.
[12] Q. Zhou, K.-Q. Xia, Universality of local dissipation scales in buoyancy-driven turbulence, Phys. Rev. Lett., 104 (2010) 124301.
[13] K. Xia, Q. Zhou, Local Dissipation Scales and Integral-Scale Reynolds Number Scalings in Thermally-Driven Turbulence, Journal of Physics: Conference Series, 318 (2011) 042016.
[14] X. Qiu, Y.L. Liu, Q. Zhou, Local dissipation scales in two-dimensional Rayleigh-Taylor turbulence, Phys. Rev. E, 90 (2014) 043012-043012.
[15] K.N. Morshed, S.K. Venayagamoorthy, L.P. Dasi, Intermittency and local dissipation scales under strong mean shear, Phys. Fluids, 25 (2013) 011701.
[16] S.C.C. Bailey, B.M. Witte, On the universality of local dissipation scales in turbulent channel flow, J. Fluid Mech., 786 (2016) 234-252.
[17] J. Mi, M. Xu, T. Zhou, Reynolds number influence on statistical behaviors of turbulence in a circular free jet, Phys. Fluids, 25 (2013) 075101.
[18] P.E. Dimotakis, Turbulent mixing, Annu. Rev. Fluid Mech., 37 (2005) 329-356.
[19] C.M. Crispo, C.S. Greco, F. Avallone, G. Cardone, On the flow organization of a chevron synthetic jet, Exp. Therm. Fluid Sci., 82 (2017) 136-146.
[20] Y. Zeng, T.H. New, T.L. Chng, Flow behaviour of turbulent nozzle jets issuing from bevelled collars, Exp. Therm. Fluid Sci., 35 (2011) 1555-1564.
[21] C.X. Thong, B.B. Dally, C.H. Birzer, P.A.M. Kalt, E.R. Hassan, An experimental study on the near flow field of a round jet affected by upstream multi-lateral side-jet, Exp. Therm. Fluid Sci., 82 (2017) 198-211.

[22] C.G. Ball, H. Fellouah, A. Pollard, The flow field in turbulent round free jets, Prog. Aero. Sci., 50 (2012) 1-26.

[23] J. Mi, R.A. Antonia, Effect of large-scale intermittency and mean shear on scaling-range exponents in a turbulent jet, Phys. Rev. E, 6402 (2001) 026302.

[24] J. Zhang, M. Xu, J. Mi, Large eddy simulations of a circular orifice jet with and without a cross-sectional exit plate, Chin. Phys. B, 23 (2014).

[25] M. Xu, A. Pollard, J. Mi, F. Secretain, H. Sadeghi, Effects of Reynolds number on some properties of a turbulent jet from a long square pipe, Phys. Fluids, 25 (2013) 035102.

[26] H. Fellouah, A. Pollard, The velocity spectra and turbulence length scale distributions in the near to intermediate regions of a round free turbulent jet, Phys. Fluids, 21 (2009) 115101-115109.

[27] J. Mi, M. Xu, C. Du, Digital filter for hot-wire measurements of small-scale turbulence properties, Meas. Sci. Technol., 22 (2011) 125401.

[28] R. Hearst, O. Buxton, B. Ganapathisubramani, P. Lavoie, Experimental estimation of fluctuating velocity and scalar gradients in turbulence, Expt. Fluids, 53 (2012) 925-942.

[29] J. Mi, R.A. Antonia, Vorticity characteristics of the turbulent intermediate wake, Expt. Fluids, 20 (1996) 383-392.

[30] J. Wyngaard, Measurement of small-scale turbulence structure with hot wires, Journal of Physics E: Scientific Instruments, 1 (1968) 1105-1108.

[31] H. Sadeghi, P. Lavoie, A. Pollard, Scale-by-scale budget equation and its self-preservation in the shear-layer of a free round jet, Int. J. Heat Fluid Flow, (2016) 85-95.

[32] C. Renner, J. Peinke, R. Friedrich, Experimental indications for Markov properties of small-scale turbulence, J. Fluid Mech., 433 (2001) 383-409.

[33] R.E. Falco, C.P. Gendrich, The turbulence burst detection algorithm of Z. Zaric, New York, Hemisphere Publishing Corp, 1990.

[34] J. Zhang, M. Xu, A. Pollard, J. Mi, Effects of external intermittency and mean shear on the spectral inertial-range exponent in a turbulent square jet, Phys. Rev. E, 87 (2013) 053009.

[35] M. Khashehchi, A. Ooi, J. Soria, I. Marusic, Evolution of the turbulent/non-turbulent interface of an axisymmetric turbulent jet, Expt. Fluids, 54 (2013) 1-12.

[36] J. Westerweel, C. Fukushima, J.M. Pedersen, J.C.R. Hunt, Mechanics of the Turbulent-Nonturbulent Interface of a Jet, Phys. Rev. Lett., 95 (2005) 174501.

[37] R. Anand, B. Boersma, A. Agrawal, Detection of turbulent/non-turbulent interface for an axisymmetric turbulent jet: evaluation of known criteria and proposal of a new criterion, Exp. Fluids, 47 (2009) 995-1007.

Highlights in our research: In this work, we systematically investigated local dissipation scales in turbulent jets:

- The work reports a PDF analysis of the local dissipation scales in turbulent jets.
- The smallest-scale dissipation fluctuations behave universally in full turbulence.
  - The universality is broken in partial turbulence where large-scale intermittency occurs.